

# Linking the loading dependence of the Maxwell–Stefan diffusivity of linear alkanes in zeolites with the thermodynamic correction factor

R. Krishna \*, J.M. van Baten

*Van 't Hoff Institute for Molecular Sciences, University of Amsterdam, Nieuwe Achtergracht 166, 1018 WV Amsterdam, The Netherlands*

Received 28 November 2005; in final form 9 January 2006

Available online 3 February 2006

## Abstract

Molecular dynamics simulations have been carried out to determine the Maxwell–Stefan diffusivity  $\mathcal{D}$  of C1–C4 linear alkanes for a range of molecular loadings,  $q$ , in AFI, MOR, MTW, and MFI zeolites. Configurational-Bias Monte Carlo simulations were used to determine the thermodynamic correction factor,  $\Gamma \equiv \partial \ln f / \partial \ln q$ . For diffusion in the large 1D pores of AFI,  $\mathcal{D}$  is proportional to  $1/\Gamma$ . In other zeolite topologies with smaller pore sizes, though such a direct proportionality is not observed, the  $\mathcal{D}$ – $q$  dependence appears to be closely linked to the  $1/\Gamma$ – $q$  characteristics, especially when the latter exhibits strong inflection.

© 2006 Elsevier B.V. All rights reserved.

## 1. Introduction

Due to their regular nanometer sized pore structures, zeolites are widely used as catalysts and adsorbents that rely on either molecular sieving principles or subtle entropy effects for achieving high selectivities in separation and reaction applications [1–3]. For the design of catalytic and separation processes employing zeolites it is necessary to have accurate information on the Fick diffusivity  $D$  of guest molecules, defined for one-component diffusion by [4]

$$\mathbf{N} = -\rho D \nabla q \quad (1)$$

where  $\mathbf{N}$  is the molar flux,  $q$  is molecular loading expressed in moles/kg, and  $\rho$  is the framework density expressed as  $\text{kg/m}^3$ . In the alternative Maxwell–Stefan (M–S) approach [4–6] the chemical potential gradient  $\nabla \mu$  is used as the driving force and the M–S diffusivity  $\mathcal{D}$  is defined by

$$\mathbf{N} = -\rho q \mathcal{D} \frac{1}{RT} \nabla \mu \quad (2)$$

where  $R$  is the gas constant,  $T$  is the temperature. The Fick and M–S diffusivities are inter-related

$$D = \mathcal{D} \Gamma \quad (3)$$

where  $\Gamma$  is the thermodynamic correction factor

$$\Gamma \equiv \frac{d \ln f}{d \ln q} \quad (4)$$

The thermodynamic factor  $\Gamma$  can be determined from knowledge of the adsorption isotherm that relates the molecular loading  $q$  to the bulk gas fugacity  $f$ . If the adsorption can be described by a single-site Langmuir model, then

$$\Gamma = \frac{1}{1 - q/q_{\text{sat}}} = \frac{1}{1 - \theta} \quad (5)$$

where  $q_{\text{sat}}$  is the saturation loading capacity and  $\theta \equiv q/q_{\text{sat}}$  is the fractional occupancy.

In general, both Fick and M–S diffusivities are dependent on the loading  $q$  and this dependence is determined inter alia by molecule–molecule interactions, zeolite topology and connectivity as evidenced by both MD simulations and experiments [7–15]. An important advantage of the M–S formulation is that factors related to adsorption thermodynamics are ‘factored’ out and therefore the  $\mathcal{D}$  is more amenable to simple interpretation in terms of hopping of molecules from one adsorption site to another. A molecule can only hop to another site when the recipient site is

\* Corresponding author. Fax: + 31 20 5255604.  
E-mail address: [r.krishna@uva.nl](mailto:r.krishna@uva.nl) (R. Krishna).

vacant and therefore in the absence of intermolecular interactions we may expect

$$\mathcal{D} = \mathcal{D}(0)(1 - \theta) \quad (6)$$

where the M–S diffusivity  $\mathcal{D}(0)$  at zero loading can be expected to be proportional to the jump frequency and the square of the mean jump distance between sites. For diffusion of 2-methylhexane that hops from one intersection site to another within the MFI framework, Kinetic Monte Carlo simulations [16] have demonstrated the validity of Eq. (6). For FAU, that has cages separated by large 0.74 nm sized windows, MD simulations [15,17,18] for a variety of alkanes in FAU have shown that the occupancy dependence of  $\mathcal{D}$  follows Eq. (6). This suggests that intermolecular interactions do not play a significant role in influencing the loading dependence of the  $\mathcal{D}$ .

From Eq. (5) we note that the fractional vacancy  $(1 - \theta)$  equals the inverse of the thermodynamic factor and therefore we may expect  $\mathcal{D}$  to be proportional to  $1/\Gamma$  for the more general case in which the adsorption isotherm does not conform to the single-site Langmuir model. For diffusion of C5–C8 alkanes in MFI an inflection in the loading dependence of  $\mathcal{D}$  is observed and this is traced to an inflection in the sorption isotherm, described by a dual-site Langmuir model [13].

Often the sorption isotherm cannot be represented either by a single-site or even dual-site Langmuir model. In such cases the thermodynamic factor needs to be determined by numerical differentiation of the adsorption isotherm. Alternatively,  $\Gamma$  can be determined from molecular simulations using the fluctuation formula derived by Reed and Ehrlich [19]

$$\Gamma = \frac{\langle N \rangle}{\langle N^2 \rangle - \langle N \rangle^2} \quad (7)$$

where  $N$  represents the number of molecules in the simulation box and  $\langle \dots \rangle$  denotes ensemble averaging. This fluctuation formula has been recently used in Monte Carlo simulations of adsorption in zeolites [20].

In this Letter we investigate the loading dependence of the M–S diffusivity  $\mathcal{D}$  for linear alkanes, in the 1–4 C atom range, in one-dimensional channels of AFI, MOR and MTW using MD simulations. We shall demonstrate that the  $\mathcal{D}$  vs.  $q$  behavior is strongly influenced by  $1/\Gamma$  vs.  $q$ . For comparison purposes we also present diffusion data for MFI that has intersecting channels structure.

## 2. CBMC and MD simulations

CBMC and MD simulations have been carried out to study adsorption and diffusion of methane (C1), ethane (C2), propane (C3), and *n*-butane (*n*C4) in AFI, MOR, MTW and MFI zeolites. Fig. 1 shows the landscapes of these zeolite topologies; the unit cell dimensions and crystallographic data are available elsewhere [21,22]. For both adsorption and diffusion simulations we use the united atom model. The zeolite framework is considered to be rigid. We consider the  $\text{CH}_x$  groups as single, chargeless interaction centers with their own effective potentials. The beads in the chain are connected by harmonic bonding potentials. A harmonic cosine bending potential models the bond bending between three neighboring beads, a Ryckaert-Bellemans potential controls the torsion angle. The beads in a chain separated by more than three bonds interact with each other through a Lennard-Jones potential. The Lennard-Jones potentials are shifted and cut at 1.2 nm. Configurational-Bias Monte Carlo (CBMC) simulations were used to determine the sorption loadings and also thermodynamic factor  $\Gamma$  by use of the Reed–Ehrlich fluctuation formula (7). The CBMC simulation details,

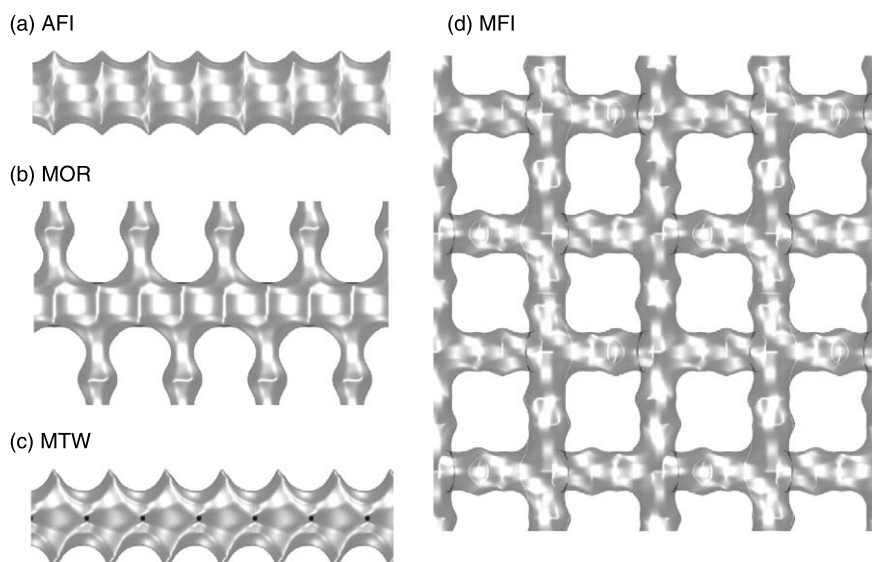


Fig. 1. Energy landscapes for (a) AFI, (b) MOR, (c) MTW, and (d) MFI zeolites.

along with the force fields have been given in our earlier publication [23]. The simulation box sizes were  $2 \times 2 \times 10$ ,  $2 \times 2 \times 8$ ,  $1 \times 20 \times 1$ , and  $2 \times 2 \times 4$  unit cells, respectively, for AFI, MOR, MTW, and MFI; it was verified that the size of the simulation box was large enough to yield reliable data on adsorption and diffusion. Periodic boundary conditions were employed.

Diffusion in a system of  $N$  molecules is simulated using Newton's equations of motion until the system properties, on average, no longer change in time. The Verlet algorithm is used for time integration. The energy drift of the entire system is monitored to ensure that the time steps taken were not too large. A time step of 1 fs was used in all simulations. For each simulation, initializing CBMC moves are used to place the molecules in the domain, minimizing the energy. Next, a fixed number of MD initialization cycles are performed, at which velocities are scaled each cycle to the temperature. This is followed by a fixed number of equilibrium MD cycles. During the equilibrium cycles, statistics are not updated, and the velocities are no longer scaled at each cycle. After a fixed number of initialization and equilibrium steps, the MD simulation production cycles start. For every cycle, the statistics for determining the mean square displacements (MSDs) are updated. The MSDs are determined for time intervals ranging from 2 fs to 1 ns. In order to do this, an order- $N$  algorithm, as detailed in Chapter 4 of Frenkel and Smit [24] is implemented. The details on how diffusivities are determined from the MSDs are to be found in Frenkel and Smit [24]. The Nosé-Hoover thermostat is used to maintain constant temperature conditions.

The Maxwell–Stefan diffusivity was determined for each of the coordinate directions

$$\bar{D} = \frac{1}{2} \lim_{\Delta t \rightarrow \infty} \frac{1}{N} \frac{1}{\Delta t} \left\langle \left( \sum_{i=1}^N (\mathbf{r}_i(t + \Delta t) - \mathbf{r}_i(t)) \right)^2 \right\rangle \quad (8)$$

where  $\mathbf{r}_i(t)$  is the position of molecule  $i$  at any time  $t$  and  $N$  is the number of molecules. For AFI and MOR, the reported diffusivities are for the  $z$ -direction, while for MTW the diffusivity along the  $y$ -direction is reported.

For MFI, the average values calculated according to  $\bar{D} = (\bar{D}_x + \bar{D}_y + \bar{D}_z)/3$  are presented. In all cases reported here, the MSD values were linear in  $t$  and we found no evidence of single file diffusion characteristics.

### 3. Simulation results

First let us consider adsorption and diffusion of C1, C2, C3 and  $n$ C4 in AFI that has 1D channels of 0.73 nm in the  $z$ -direction. The CBMC simulations of pure component isotherms are shown in Fig. 2a. Our CBMC simulation methodology [23], yields the molar loadings as functions of the bulk gas fugacity  $f$ . For none of the molecules were we able to fit the isotherms to either a single-site or dual-site Langmuir model with good accuracy. The MD simulation results for the M–S  $\bar{D}$  are normalized with respect to the zero-loading values  $\bar{D}(0)$ , and presented along with the corresponding values of  $1/\Gamma$  in Fig. 2b–e. For all four alkanes there is good agreement between the loading dependences of  $\bar{D}/\bar{D}(0)$  and of  $1/\Gamma$ . Of particular note is the slight inflection in  $1/\Gamma$  for C1 at  $q \approx 2.8$ ; this inflection behavior is also manifested in the dependence of  $\bar{D}$  on  $q$ . An important consequence of diffusion data for linear alkanes in AFI presented here is that in view of Eq. (3) the Fick diffusivity  $D$  will be practically independent of  $q$ . This is a convenient result from a practical point of view.

The corresponding data for MOR are shown in Fig. 3. For MOR, the diffusion is along the 12-ring channels running in the  $z$ -direction; the channel size is 0.65–0.7 nm, smaller than for AFI. For both C1 and C2 there is good match between the loading dependences of  $\bar{D}$  and of  $1/\Gamma$ . As was the case for C1 in AFI, the  $1/\Gamma$  data for C1 in MOR shows an inflection at  $q \approx 2.8$ ; this inflection behavior is also reflected in the  $\bar{D}$  vs.  $q$  data. For C3 and  $n$ C4 diffusion in MOR, however, the  $\bar{D}/\bar{D}(0)$  values fall less sharply than  $1/\Gamma$  does; this is due to the reduction in the energy barrier for diffusion with increased loading, as discussed earlier [17]. For C3, the minimum in  $1/\Gamma$  at  $q \approx 1.1$  leads to a corresponding minimum in  $\bar{D}$ .

The sorption and diffusion data for MTW are shown in Fig. 4. For MTW, the diffusion is along the  $y$ -direction and

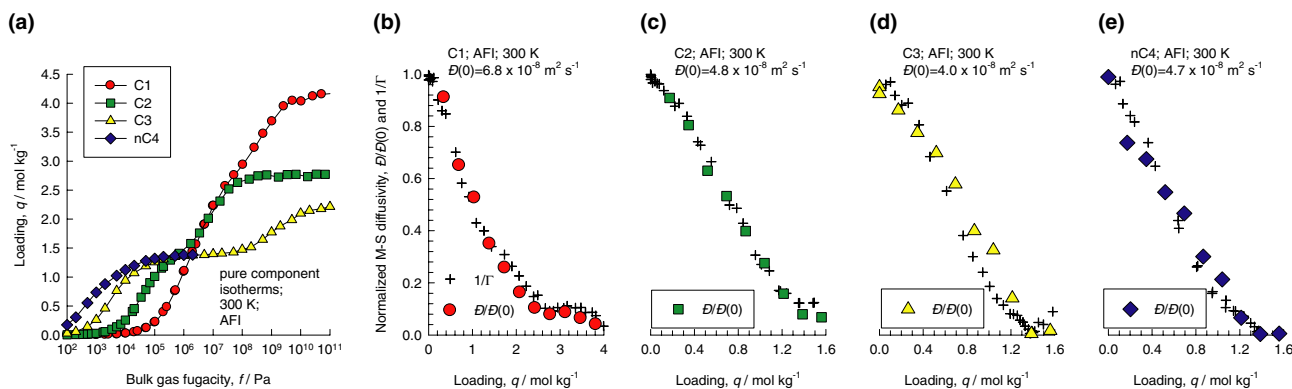


Fig. 2. (a) CBMC simulations of pure component isotherms in AFI of C1, C2, C3 and  $n$ C4. MD simulation data (filled symbols) for normalized M–S diffusivity  $\bar{D}/\bar{D}(0)$  in AFI of (b) C1, (c) C2, (d) C3, and (e)  $n$ C4. Also shown by pluses are the corresponding data on  $1/\Gamma$ .

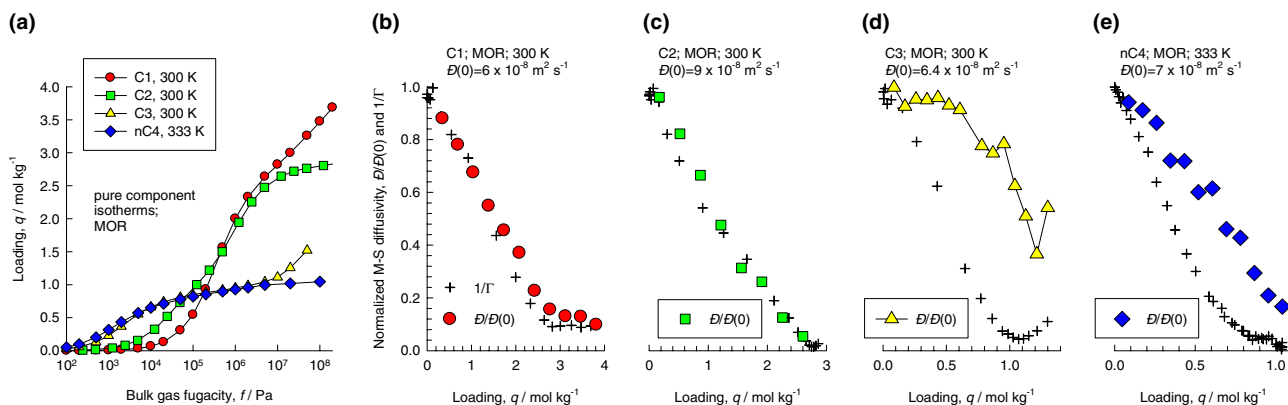


Fig. 3. (a) CBMC simulations of pure component isotherms in MOR of C1, C2, C3 and *n*C4. MD simulation data (filled symbols) for normalized M–S diffusivity  $\mathcal{D}/\mathcal{D}(0)$  in MOR of (b) C1, (c) C2, (d) C3, and (e) *n*C4.

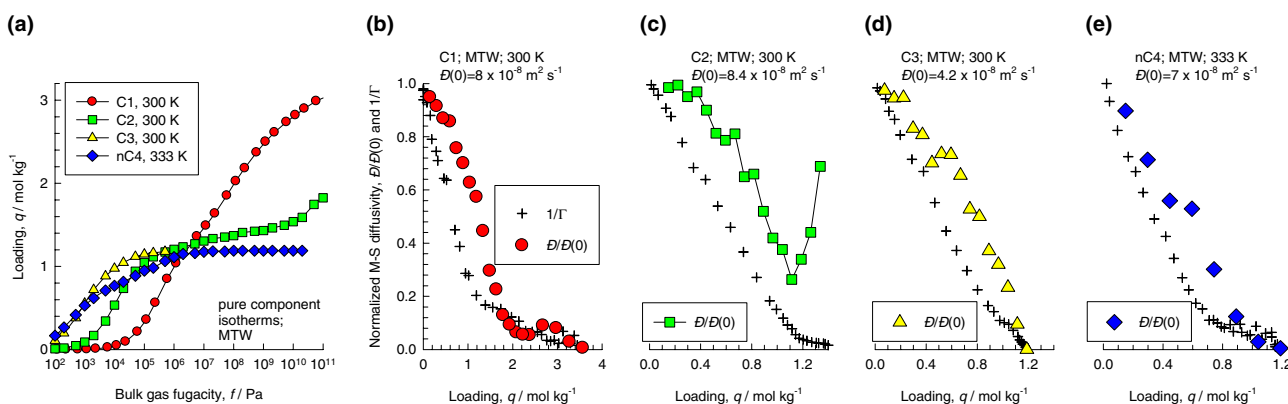


Fig. 4. (a) CBMC simulations of pure component isotherms in MTW of C1, C2, C3 and *n*C4. MD simulation data (filled symbols) for normalized M–S diffusivity  $\mathcal{D}/\mathcal{D}(0)$  in MTW of (b) C1, (c) C2, (d) C3, and (e) *n*C4.

the channel size is 0.56–0.6 nm, smaller than for MOR. For C1 there is a reasonable correlation between the loading dependences of  $\mathcal{D}$  and of  $1/\Gamma$ , and there is inflection in both  $\mathcal{D}$  and  $1/\Gamma$  at  $q \approx 2$ . For C2, the slight inflection in  $1/\Gamma$  at  $q \approx 1.2$  appears to have a disproportionately large influence on  $\mathcal{D}$ , that shows a sharp minimum at this loading; the precise reasons for this are unclear. The diffusion

behavior of C3 and *n*C4 in MTW show a similar behavior as in MOR; the  $\mathcal{D}/\mathcal{D}(0)$  values fall less sharply than  $1/\Gamma$  does.

For comparison purposes, data on sorption and diffusion in the intersecting channels of MFI zeolite, with channel sizes 0.51–0.56 nm, are shown in Fig. 5. For all molecules the  $\mathcal{D}/\mathcal{D}(0)$  values fall less sharply than  $1/\Gamma$ .

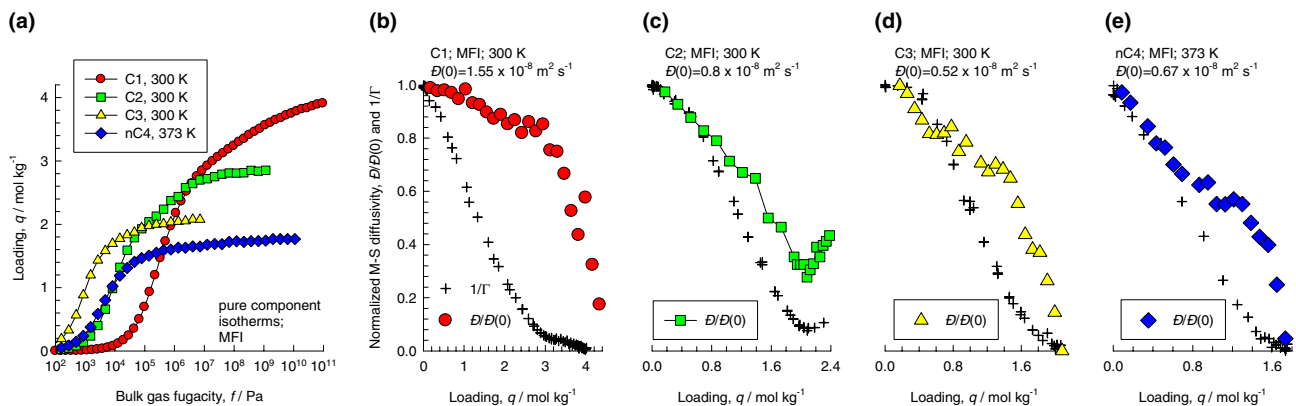


Fig. 5. (a) CBMC simulations of pure component isotherms in MFI of C1, C2, C3 and *n*C4. MD simulation data (filled symbols) for normalized M–S diffusivity  $\mathcal{D}/\mathcal{D}(0)$ s in MFI of (b) C1, (c) C2, (d) C3, and (e) *n*C4.

An explanation for the loading dependence of  $\bar{D}$  of C1 is given by Beerdsen et al. [25]; increased loading alters the energy barrier for diffusion and this influence is non-linear. For C2, the slight inflection in  $1/\Gamma$  at  $q \approx 2$  causes a sharp minimum in the value of  $\bar{D}$ ; this inflection has been noted earlier by Chong et al. [11], and appears to be analogous to the behavior of C2 in MTW, and of C3 in MOR. The diffusion of C3 and  $n$ C4 in MFI show a behavior similar to that for these molecules in MOR and MTW; the  $\bar{D}/\bar{D}(0)$  values fall less sharply than does  $1/\Gamma$  with  $q$ .

#### 4. Conclusions

In this Letter we have investigated the loading dependence of the M–S diffusivity  $\bar{D}$  of C1–C4 linear alkanes in four zeolite structures. The pore size of the zeolite appears to have a major influence on the  $\bar{D}$  vs.  $q$  characteristics. For large pore AFI, the  $\bar{D}$  is proportional to  $1/\Gamma$ . This proportionately also holds for C1 and C2 diffusion in MOR, that has slightly smaller pore size than AFI. For all other guest–host combinations reported here,  $\bar{D}/\bar{D}(0)$  values fall less sharply with  $q$  than  $1/\Gamma$ , suggesting that the energy barrier for diffusion is influenced by the molecular loading [10,15,17,25]. In all cases whenever  $\bar{D}$  vs.  $q$  exhibits an inflection, this can be traced to an inflection in  $1/\Gamma$  vs.  $q$ . Further work is required in order to develop guidelines to predict the loading dependence of the M–S diffusivity for various guest–host combinations.

#### Acknowledgments

We acknowledge (a) receipt of TOP subsidy from the Netherlands Foundation for Fundamental Research (NWO-CW) for intensification of reactors, (b) D. Dubbeldam, S. Calero, T.J.H. Vlught, E. Beerdsen and B. Smit for providing the CBMC and MD simulation codes, and (c)

NWO/NCF for provision of high performance computing resources.

#### References

- [1] R. Krishna, B. Smit, S. Calero, Chem. Soc. Rev. 31 (2002) 185.
- [2] B. Smit, R. Krishna, Chem. Eng. Sci. 58 (2003) 557.
- [3] R. Krishna, R. Baur, Chem. Eng. Sci. 60 (2005) 1155.
- [4] R. Krishna, R. Baur, Sep. Purif. Technol. 33 (2003) 213.
- [5] F.J. Keil, R. Krishna, M.O. Coppens, Rev. Chem. Eng. 16 (2000) 71.
- [6] A.I. Skoulidas, D.S. Sholl, R. Krishna, Langmuir 19 (2003) 7977.
- [7] H. Jobic, J. Kärger, M. Bée, Phys. Rev. Lett. 82 (1999) 4260.
- [8] G.K. Papadopoulos, H. Jobic, D.N. Theodorou, J. Phys. Chem. B 108 (2004) 12748.
- [9] A.I. Skoulidas, D.S. Sholl, J. Phys. Chem. A 107 (2003) 10132.
- [10] R. Krishna, D. Paschek, R. Baur, Micropor. Mesopor. Mater. 76 (2004) 233.
- [11] S.S. Chong, H. Jobic, M. Plazanet, D.S. Sholl, Chem. Phys. Lett. 408 (2005) 157.
- [12] R. Krishna, J.M. van Baten, D. Dubbeldam, J. Phys. Chem. B 108 (2004) 14820.
- [13] R. Krishna, J.M. van Baten, Chem. Phys. Lett. 407 (2005) 159.
- [14] R. Krishna, J.M. van Baten, Chem. Eng. Technol. 28 (2005) 160.
- [15] R. Krishna, J.M. van Baten, J. Phys. Chem. B 109 (2005) 6386.
- [16] D. Paschek, R. Krishna, Phys. Chem. Chem. Phys. 2 (2000) 2389.
- [17] J.M. van Baten, R. Krishna, Micropor. Mesopor. Mater. 84 (2005) 179.
- [18] S. Chempath, R. Krishna, R.Q. Snurr, J. Phys. Chem. B 108 (2004) 13481.
- [19] D.A. Reed, G. Ehrlich, Surf. Sci. 102 (1981) 588.
- [20] H. Chen, D.S. Sholl, Langmuir 22 (2006) 709.
- [21] C. Baerlocher, L.B. McCusker, Database of zeolite structures, International Zeolite Association, Available from <http://www.iza-structure.org/databases/>, 12 October 2004.
- [22] J.M. van Baten, R. Krishna, MD simulations of diffusion in zeolites, University of Amsterdam, Available from <http://www.science.uva.nl/research/cr/md/>, 1 November 2004.
- [23] D. Dubbeldam, S. Calero, T.J.H. Vlught, R. Krishna, T.L.M. Maesen, B. Smit, J. Phys. Chem. B 108 (2004) 12301.
- [24] D. Frenkel, B. Smit, Understanding Molecular Simulations: from Algorithms to Applications, Academic Press, San Diego, 2002.
- [25] E. Beerdsen, D. Dubbeldam, B. Smit, Phys. Rev. Lett. 95 (2005) 164505.